AG10 inhibits amyloidogenesis and cellular toxicity of the familial amyloid cardiomyopathy associated V122I transthyretin

Sravan C. Penchala[a,1], Stephen Connelly[b,c,1], Yu Wang[a,1], Miki S. Park[a], Lei Zhao[c], Aleksandra Baranczak[c], Irit Rappley[c], Hannes Vogel[d], Michaela Liedtke[d], Ronald M. Witteles[e], Evan T. Powers[c], Natàlia Reixach[c], William K. Chan[a], Ian A. Wilson[b], Jeffery W. Kelly[c], Isabella A. Graef[d,2], and Mamoun M. Alhamadsheh[a,2]

[a]Department of Pharmaceutics & Medicinal Chemistry, University of the Pacific, Stockton, California, USA.

[b]Departments of Integrative Structural and Computational Biology and [c]Molecular and Experimental Medicine, The Scripps Research Institute, La Jolla, California, USA.

[d]Department of Pathology and [e]Division of Cardiovascular Medicine, Stanford University School of Medicine, Stanford, CA, USA

[1]These authors contributed equally to this work.

[2]To whom correspondence should be addressed. E-mail: malhamadsheh@pacific.edu or igraef@stanford.edu

Supplementary Information

Supplementary Text:

Subunit Exchange Assay: We used subunit exchange assays to determine the binding constants of **AG10** and tafamidis to V122I-TTR and also to evaluate cooperativity between the two TTR T_4 sites (Fig. S8). This assay is based on TTR's dynamic tetramerization equilibrium: TTR tetramers are constantly in a process of dissociating and then re-associating. Thus, a mixture of unlabeled homotetramers and FLAG-tagged homotetramers will slowly equilibrate to a statistical distribution of homo- and heterotetramers that can be separated and quantified by ion exchange chromatography. The dissociation of the tetramer is the rate-limiting step in the TTR aggregation process , and is inhibited by small molecules that bind to one or both of TTR's T_4 binding sites and, thus, stabilizing the tetramers. The extent of inhibition depends on the fraction of TTR that does not have any small molecules bound to it, and therefore on the small molecule's dissociation constants with TTR. Mixtures consisting in equimolar amounts of recombinant untagged and FLAG-tagged TTR (total TTR final concentration 0.45 uM) were prepared and incubated in the presence of 0, 0.25, 0.5, 1.0, 1.5, and 2.0 molar equivalents (relative to total TTR tetramer) of tafamidis or **AG-10**. Subunit exchange was monitored over a period of 32 to 48 hours, a sufficient amount of time for V122I-TTR to completely exchange subunits in the absence of small molecules. Increasing amounts of both tafamidis and **AG-10** progressively decreased the subunit exchange rate. A global fit of the subunit exchange data for both compounds yielded K_{d1} = 6.2 ± 2.0 nM and K_{d2} = 139 ± 80 nM for **AG-10**. For tafamidis, the fit yielded K_{d1} = 8.1 ± 0.8 nM, but K_{d2} was too high to be accurately fit at such a low TTR concentration; we estimate the lower bound on K_{d2} to be around 1 μM.

Probe 3 Assay in Buffer: In addition to selectivity, negative cooperative binding to TTR (K_{d2} higher than K_{d1}), which many TTR ligands display, might affect competition with probe **3** in this assay. Dissociation of a ligand from the low affinity site could permit probe **3** to bind and subsequently react, rendering the remaining candidate kinetic stabilizer binding site the low affinity site. To distinguish, whether differences between ligands in displacing **3** from TTR, are due to differences in binding selectivity or negative cooperativity, one can compare displacement of **3** by a ligand from recombinant TTR (no other competing proteins present) to displacement of **3** from serum TTR (~4000 other proteins present). The probe **3** ligand competition assay was repeated as described in the main text, but in phosphate buffer (pH 7.0, 10 mM sodium phosphate, 10 mM KCl, 1 mM EDTA) with added recombinant WT-TTR (3.6 μM; Fig. S10). As we have seen in the serum assay (Fig. 3A and 3B), diflunisal has the lowest selectivity and the highest negative cooperativity (99.0 ± 5.6% in buffer) and performs worst, whereas the environmental toxin polychlorinated biphenyl **(PCB)**, which is proposed to bind TTR with no cooperativity ($K_{d1} = K_{d2} = 3$ nM) performs best (1). **AG10** exhibits modestly negative cooperative ($K_{d1} = 4.8$ nM and $K_{d2} = 314$ nM) binding and binds with high selectivity, thus it performs well (15.5 ± 2.9% probe binding in buffer). Molecules displaying negative cooperative binding like tafamidis ($K_{d1} = 4.4$ nM and $K_{d2} = 280$ nM) are predicted to perform poorly in this assay even though tafamidis exhibits selectivity for TTR in serum (54.2 ± 6.5% in buffer) (2, 3). Therefore, while it is clear that **AG10** is more selective to serum TTR than tafamidis, the results of the assay are not inconsistent with the previously established result that tafamidis occupies at least one of the two binding sites on TTR (i.e. tafamidis exhibits a binding stoichiometry of 0.8 out of maximum of 2) (3).

The results of the ligand competition assay in serum have previously been shown to correlate with the results of an immunoprecipitation-based assay that directly measures selectivity (see main text) (4). The data are re-plotted here (from Choi et al. (4))for the reader's convenience (Fig. S11) and the equation for the line of best fit is:

Equivalents of small molecule bound =

$$1.55\ (\pm 0.05) - 0.015\ (\pm 0.001) \times (\%\ \text{TTR-probe } \mathbf{3} \text{ fluorescence at 3 h relative to control})$$

AG10 protects human cardiomyocytes from TTR-induced cytotoxicity. Since there is no animal model for TTR amyloid cardiomyopathy that reproduces the pathophysiology observed in FAC patients, we turned to a recently developed *in vitro* cell-based assay. This cellular model, which uses the human cardiac cell line AC16, is currently the pathophysiologically most relevant tissue culture model for SSA and FAC (5). Treatment of AC16 cells with the destabilized V122I-TTR (8 μM) variant decreased cell viability (43.0 ± 8.6% viability) relative to vehicle treated cells (100% viability) (Fig. S13). TTR incubated with 8 μM of diflunisal provided partial protection for the AC16 cells from the proteotoxicity of amyloidogenic V122I-TTR (70.1 ± 4.3% viability). At 8 μM, both **AG10** and tafamidis prevented the cytotoxic effects of V122I-TTR towards AC16 cells (Fig. S13).

AG10 is chemically stable. To test whether **AG10** might be suitable for oral administration, we tested its chemical stability in simulated gastric fluids and found that **AG10** was stable up to 24 hours (Fig. S15).

AG10 has good metabolic stability *in vitro*. Incubation of **AG10** with human liver microsomes (HLM) provides information regarding metabolic stability and also gives early guidance relating to drug half-life. **AG10** was stable when tested with HLM (only 10% of **AG10** was metabolized after 90 min).

AG10 has no cytotoxic effects. The effect of **AG10**, compound **1**, and tafamidis on the viability and proliferation of four cell lines was studied via the (3-(4,5-dimethylthiazol-2-yl)-2,5-diphenyltetrazolium bromide (MTT) assay (Fig. S16). Compounds were added to the culture medium at different concentrations (concentration range from 1 to 100 μM) and the cells were incubated for additional 24 h at 37 °C. **AG10** showed no cytotoxic effects towards any of the cell lines that were tested. Similar results were obtained for tafamidis, which at high concentrations had only minor cytotoxic effects against MCF7 cells. At high concentrations (>50 μM) compound **1** displayed toxic effects towards Hela and Hep3B cells.

MDCK permeability assay for AG10 *in vitro*. MDCK epithelial cell monolayer transport assay, a commonly used general model to predict drug transport from the intestinal lumen into the bloodstream, was employed to study the apparent permeability of **AG10** *in vitro*. The transport of **AG10** across MDCK cells was studied in both directions, apical to basolateral (A→B; represents the transport of drug from intestinal into the bloodstream) and basolateral to apical (B→A; represents the efflux of drug from bloodstream to the intestinal lumen). The A→B permeability (P_{app}) of **AG10** (at 200 μM) in MDCK cell monolayer assay was found to be 8.1 x 10^{-7} cm/s and the B→A was about 3.9 x 10^{-7} cm/s. The ratio of B→A P_{app} to A→B P_{app} is designated as the efflux ratio and was ~ 0.5 for **AG10**. This value suggests that **AG10** would have acceptable permeability across the intestinal epithelia.

Oral bioavailability and preliminary pharmacokinetics of AG10 in mice. Our initial ADME studies (performed by Medicilon Inc., an FDA approved CRO that is specialized in preclinical evaluation) show that **AG10** has favorable drug-like properties. Following intravenous injection of **AG10** into mice, the compound was eliminated with first-order kinetics over 24 h ($t_{1/2}$ ~ 4.8 hours) (Fig. 14 and Table S2). We also found that **AG10** was orally bioavailable and absorbed within 5 min after oral gavage. After a single dose, **AG10** was still present in the circulation at 24 h ($t_{1/2}$ ~ 42.3 hours).

Materials and methods:

Prealbumin from human plasma (human TTR) was purchased from Sigma. Diflunisal, Thyroxine (T_4), and resveratrol were purchased from Fisher. ^{1}H NMR and ^{13}C NMR spectra were recorded on a Jeol JNM−ECA600 spectrometer and calibrated using residual undeuterated solvent as an internal reference. High resolution mass spectra (HRMS) were determined by JEOL AccuTOF DART using Helium as an ionization gas and polyethylene glycol (PEG) as an external calibrating agent. HPLC analysis was performed on a Waters™ Alliance 2790 system attached to Waters™ 2990 PDA detector operating between the UV ranges of 200 – 400 nm. Empower 2.0 data acquisition system was used for quantification purposes. A Waters™ XBridge C18 column with L1 packing (4.6 X 150 mm, 5μm) was used at ambient temperature. The mobile phase was composed of 23 % (v/v) acetonitrile in an aqueous solution containing 50mM potassium phosphate (pH 3.2). An isocratic separation was performed for 30 min at a flow rate of 0.5 mL/ min. A small volume of 40 μL injection of each standard and/or sample was performed to obtain the chromatogram. The UV absorbance was recorded at 240 nm. Wild-type TTR concentration in serum was measured using nephelometric analyzer (28 mg/dL or 5 μM).

Chemical Synthesis of AG10.

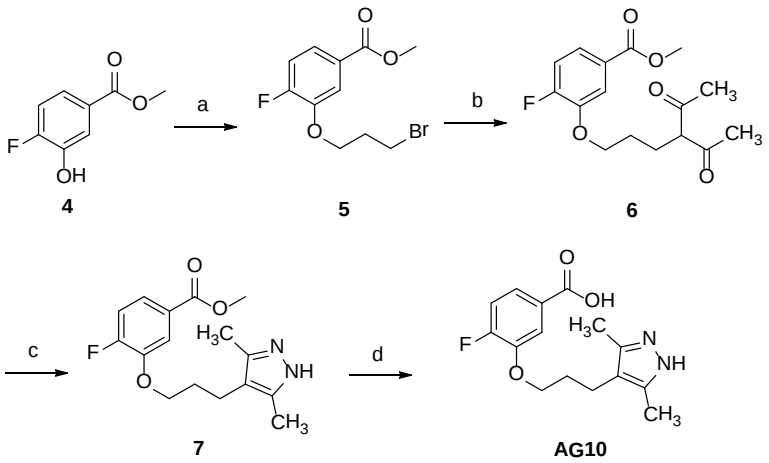

Scheme S1. Synthesis of **AG10**. a) 1,3-dibromopropane, K_2CO_3, DMF, rt, 16 hours; b) acetylacetone, 1,8-Diazabicyclo[5.4.0]undec-7-ene (DBU), benzene, rt, 3 days; c) hydrazine hydrate, ethanol, 90^{o}C, 4 hours; d) LiOH, THF, water, rt, 14 hours.

Methyl 3-(3-bromopropoxy)-4-fluorobenzoate (5); To a solution of methyl 4-fluoro-3-hydroxybenzoate **4 (**3.0 g, 17.6 mmol, 1 equiv) and 1,3-dibromopropane (9.0 ml, 88.2 mmol, 5 equiv) in DMF (40 ml) was added K_2CO_3 (2.93 g, 21.2 mmol, 1.2 equiv). The reaction mixture was stirred at room temperature for 16 hours. The mixture was diluted with EtOAc (1.5 L), washed with brine (3x0.5 L) and dried with Na_2SO_4. The solution was filtered and concentrated. The residue was purified by flash column chromatography (silica gel, 1-10% EtOAc/hexanes) to afford compound **5** (4.21 g, 82% yield); ^{1}H NMR (CD3OD, 600 MHz) δ 7.67-7.61 (m, 2H), 7.14-7.07 (m, 1H), 4.21 (t, 2H, *J* = 5.89 Hz), 3.89 (s, 3H), 3.62 (t, 2H, *J* = 6.38 Hz), 2.38-2.31 (m, 2H); (ESI$^+$) m/z: calcd for $C_{11}H_{12}BrFO_3$ + H^+ 290.00; found 290.01 (M + H^+).

Methyl 3-(3-(3,5-dimethyl-1H-pyrazol-4-yl)propoxy)-4-fluorobenzoate (7); A solution of **5** (780 mg, 2.69 mmol, 1 equiv) in benzene (3 ml) was added dropwise to a solution of acetyl acetone (0.552 ml, 5.38 mmol, 2 equiv) and DBU (0.804 ml, 5.38 mmol, 2 equiv) in benzene (7 ml). The reaction mixture was stirred at room temperature for 3 days. The mixture was filtered and concentrated. The residue was purified by flash column chromatography (silica gel, 1-10% EtOAc/hexanes) to afford compound **6** which was used in the next step directly. Hydrazine hydrate (0.36 ml, 6.73 mmol, 2.5 equiv) was added to a solution **6** in ethanol (5 ml) and the reaction was heated under reflux for 4 hours. The reaction was concentrated and purified by flash column chromatography (silica gel, 1-20% MeOH/CH_2Cl_2) to afford compound **7** (288 mg, 35% yield) in two steps; ^{1}H NMR (CD_3OD, 600 MHz) δ 7.64-7.58 (m, 2H), 7.20-7.15 (m, 1H), 4.01 (t, 2H, *J* = 6.0 Hz), 3.86 (s, 3H), 2.58 (t, 2H, *J* = 7.2 Hz), 2.12 (s, 6H), 1.97-1.92 (m, 2H); HRMS (DART) m/z: calcd for C16H19FN2O + H^+ 307.1458; found 307.1452 (M + H^+).

3-(3-(3,5-Dimethyl-1H-pyrazol-4-yl)propoxy)-4-fluorobenzoic acid (AG10); To a suspension of **7** (100 mg, 0.33 mmol, 1 equiv) in a mixture of THF (3 ml) and water (3 ml) was added LiOH.H_2O (27.5 mg, 0.66 mmol, 2 equiv). The reaction mixture was stirred at room temperature for 14 hr after which it was cooled to 0^{o}C and carefully acidified to pH 2-3 with 1N aqueous HCl. The mixture was extracted with EtOAc (3 x 30 ml) and the combined organic extracts were dried over anhydrous sodium sulfate and concentrated in vacuo. The crude product was subjected to flash column chromatography (silica

gel, 10-50% MeOH/CH_2Cl_2) to give of **AG10** (68 mg, 71% yield) as a white solid (>98% purity by HPLC); ^{1}H NMR (CD_3OD, 600 MHz) δ 7.65-7.58 (m, 2H), 7.20-7.14 (m, 1H), 4.00 (t, 2H, *J* = 6.0 Hz), 2.58 (t, 2H, *J* = 5.8 Hz), 2.12 (s, 6H), 1.97-1.92 (m, 2H); HRMS (DART) m/z: calcd for C15H17FN2O3 + H^+ 293.1301; found 293.1293 (M + H^+).

Fluorescence Polarization (FP) Binding Assay.

Determination of FP probe displacement by TTR ligands: The affinity of test compounds to TTR was determined by their ability to displace FP probe form TTR using our recently developed assay (6). The apparent binding constant was reported as the mean for triplicate experiments and the best data fit was determined by R^2 value.

Determination of IC50 using the FP assay: Serial dilutions of **AG10**, and tafamidis (100 μM to 0.003 μM) were added to a solution of FP-probe **2** and TTR in assay buffer (25 μL final volume). The FP assay was then carried out as described above.

Isothermal Titration Calorimetry (ITC). Calorimetric titration was carried out on a VP-ITC calorimeter (MicroCal, Northhampton, MA). A solution of **AG10** (25 μM in PBS pH 7.4, 100 mM KCl, 1 mM EDTA, 2.5% DMSO) was prepared and titrated into an ITC cell containing 2 μM of TTR in an identical buffer. Prior to each titration, all samples were degassed for 10 minutes. 37 injections of **AG10 (**8.0 μL each) were injected into the ITC cell (at 25^{o}C) to the point that TTR was fully saturated with ligand. Integration of the thermogram after the subtraction of blanks yielded a binding isotherm that fit best to a model of two interacting sites exhibiting negative cooperativity. The data were fit by a nonlinear least squares approach with four adjustable parameters: K_{d1}, Δ*H1*, *T*Δ*S1*, K_{d2}, Δ*H2*, and *T*Δ*S2* using the ITC data analysis module in MicroCal ORIGIN 5.0 software.

Subunit Exchange Assay. Homotetrameric untagged V122I-TTR (0 FLAG) and V122I-TTR with an N-terminal acidic FLAG tag (4 FLAG) were mixed at a concentration of 0.225 μM tetramer each (giving a total TTR concentration of 0.45 μM) in 10 mM sodium phosphate pH 7.6, 100 mM KCl, 1 mM EDTA with the desired concentration of **AG10** or tafamidis in DMSO (final concentration of DMSO was 0.5%). The reactions were incubated at 25 °C for the indicated times. Subunit exchange was measured using a Waters Acquity H-Class Bio UPLC system equipped with a fluorescence detector and using a ProteinPak Hi Res Q column. A total of 50 μL of the exchange reaction was injected onto the column, then eluted with a gradient of 240- 420 mM NaCl in 25 mM Tris pH 8.0, 1 mM EDTA. Because the FLAG tag provides ~6 negative charges to each tagged TTR subunit (at pH 7), retention time of tetramers on the anion exchange column increases with increasing numbers of FLAG-tagged subunits. Protein elution curves were followed by fluorescence at 335 nm (as is typical for TTR) due to the extremely low signal in the UV channel. Peak areas were determined by integration. The extent of exchange was calculated by dividing the area of the 2 FLAG peak by the total area under all 5 peaks. At saturation, the predicted stoichiometries for the various tetramers are 1:4:6:4:1, thus the 2 FLAG peak is predicted to represent 6/16 = 0.375 of the total peak area. The fraction exchange was calculated as (extent of exchange) / 0.375. The reported rate constants of exchange were determined from plotting the fraction exchange data in Mathematica and fitting the results to a first-order single-exponential kinetic equation.

Serum TTR Selectivity Assay. The binding affinity and selectivity of the test compounds to TTR was determined by their ability to compete for covalent probe **3** binding to TTR in human serum (Fig. S4) as previously reported (4). An aliquot of 98 μL of human serum (Sigma–Aldrich) was mixed with 1 μL of test compounds (1.0 mM stock solution in DMSO, final concentration: 10 μM) and 1 μL of probe **3** (0.36 mM stock solution in DMSO: final concentration: 3.6 μM). The fluorescence changes (λ_{ex} = 328

nm and λ_{em} = 384 nm) were monitored every 10 min using a microplate spectrophotometer reader (Molecular Devices SpectraMax M5) for 6 h at 25^{o}C.

Measurement of Serum WT-TTR Tetramer Stability against Acid Denaturation. All compounds were 10 mM stock solutions in DMSO and diluted accordingly with DMSO for different assays. 0.5 μL of each compound was added to 24.5 μL of human serum (from human male AB plasma, Sigma) to make the final concentration ranging from 0.1-50 μM. The samples were incubated at 37°C for 2 h, and then 10 μl of the samples were diluted 1:10 with either neutral pH buffer (pH 7.0, PBS, 100 mM KCl, 1 mM EDTA, 1 mM DTT) or acidification buffer (pH 4.0, 100 mM sodium acetate, 100 mM KCl, 1 mM EDTA, 1 mM DTT). The samples in neutral buffer were directly cross-linked with glutaraldehyde (final concentration of 2.5%) for 5 min, and then quenched with 10 μL of 7% sodium borohydride solution in 0.1 M NaOH, while the samples in acidification buffer were incubated at room temperature for 72 h and then cross-linked and quenched with the same protocol. All the samples were denatured with adding 100 μL SDS gel loading buffer and boiled for 5 min. 12.5 μL of each sample was separated in 12% SDS-PAGE gels and analyzed by immunoblotting using anti-TTR antiserum (DAKO A0002, 1:10,000 dilution). The density of all TTR bands was quantified using an Odyssey infrared imaging system (LI-COR Bioscience, Lincoln, NE) and reported as % TTR tetramer

Measurement of Serum V122I-TTR Tetramer Stability against Acid Denaturation
Subjects: Samples were obtained from two FAC patients with the V122I-TTR mutation. **Patient 1**; Heterozygous FAC patient; Heterozygous V122I/WT-TTR, African American, male, age 56**. Patient 2**; Homozygous FAC patient; Homozygous V122I-TTR, Caucasian, female, age: 62. Mutations confirmed by sequencing / test: 'Amyloidosis DNA titer'): (The western blot analysis was performed as described above for WT-TTR. IgG analysis was performed using IRdye800 goat anti-human IgG (1:7500 dilution, O/N incubation at 4°C, no secondary antibody needed).

Cell-based Assay. The human cardiac cell line AC16 was maintained in DMEM:F12 (1:1) supplemented with 10% FBS, 1 mM Hepes buffer, 2 mM L-glutamine, 100 units/mL penicillin and 100 μg/mL streptomycin. Two to 4-day-old cultures (~70% confluent) were used for the experiments. The cardiac AC16 cells were seeded in black wall, clear bottom, tissue culture treated 96-well plates (Costar) at a density of 300 cells/well, in 50μL of Opti-MEM supplemented with 5% FBS, 1 mM Hepes buffer, 2 mM L-glutamine, 100 units/mL penicillin and 100 μg/mL streptomycin, 0.05 mg/mL $CaCl_2$ and incubated overnight at 37°C.

Cell Assay: Recombinant amyloidogenic V122I-TTR purified in HBSS (Mediatech, Manassas, VA) was used as a cytotoxic insult to cardiac AC16 cells. Candidate compounds (10 mM stocks in DMSO) were diluted with V122I-TTR (16 μM in HBSS, filter sterilized) or with HBSS only. The mixtures were vortexed and incubated for 30 min at r.t. Additionally, HBSS and V122I-TTR (16 μM in HBSS), containing the same amount of DMSO as TTR/candidate compound mixtures, were prepared in parallel and incubated under the same conditions to serve as controls for cell viability.
After the 30 min of pre-incubation of the test compounds with V122I-TTR, 50 μL of each mixture (HBSS alone, V122I-TTR alone, V122I-TTR + compounds or compounds alone) were added to the cells and incubation proceeded for 24 h at 37°C, after which cell viability was measured. The final concentration of both V122I-TTR and compounds in the cell assay was 8 μM.

Cell viability assay: The viability of cells treated with TTR or TTR/candidate compound was evaluated by a resazurin reduction assay (5). Briefly, 10 μL/well of resazurin (500 μM, PBS) was added to each well and incubated for 2-3 h at 37 °C. Viable cells reduce resazurin to the highly fluorescent resorufin

dye, which is quantitated in a multiwell plate reader (Ex/Em 530/590nm, Tecan Safire2, Austria). Cell viability was calculated as percentage of fluorescence relative to cells treated with vehicle only (HBSS, 100% viability) after subtraction of blank fluorescence (wells without cells). All experiments were performed in at least four replicates. Averages and SEM corresponding to 2 independently performed experiments are presented.

Evaluating the effect of AG10 on COX-1, COX-2, THR, hERG, and CYP enzymes. The COX and THR assays were carried out by Cerep Laboratories in Redmond, WA. The hERG potassium ion channel assay was carried out by ChanTest Corporation, Cleveland, OH. The inhibition assays for CYP enzymes were carried out by Quintara Biosciences, South San Francisco, CA.

Stability of AG10 in Simulated Gastric Fluid. The simulated gastric fluid (SGF) was prepared according to US pharmacopeia guidelines. Briefly, SGF contains 0.2% (w/v) of sodium chloride, 0.32% (w/v) of pepsin and 0.7% (v/v) of concentrated HCl in water (final pH of 1.2). Compound **AG10** was added to the SGF (20 µM) and incubated at 37°C in a shaking water bath. Gastric stability study samples (50 µL) were assayed at 0, 2, 4 and 24 hour time intervals. Samples were processed by adding 200 µL methanol followed by centrifuging at 16000 x *g* for 5 min and analyzing the supernatant using the HPLC method above.

Metabolism Study of AG10 in Human Liver Microsomes (HLM). Microsomal incubations were conducted in triplicates. Incubation mixtures consisted of human liver microsomes (1 mg/mL), **AG10** (1 µM), $MgCl_2$ (4 mM), and NADPH (1.6 mM) in a total volume of 500 µL potassium phosphate buffer (100 mM, pH 7.4). Incubation mixtures without NADPH were preincubated at 37^{o}C for approximately 10-15 minutes then reaction was started by addition of NADPH (or buffer for negative control). At 0, 60 and 120 minutes, 80 µL aliquots were taken and added to equal volume of methanol containing 500 µM cortisone as internal standard. Samples were centrifuged at 16,000 x *g* for 10 minutes and supernatants were stored at -20^{o}C until analysis by HPLC.

Bidirectional Transport Studies in MDCK cells. MDCK cells were obtained from American Type Culture Collection (ATCC) and cultured in DMEM supplemented with 10% FBS, 10 U/ml of penicillin, and 10 µg/ml of streptomycin. Cells were grown for 3-5 days after seeding in 0.4 micron polyester six-well Trans-well permeable support from Costar. Cells were preincubated with 25 mM HEPES in Hank's Balanced salt solution (transport media) for approximately 15 min prior to transport study. Transport study was started by adding 200 µM of compound **AG10** in transport media to either the basolateral (2.5 mL) or apical side (1.5 mL). Transport media without the drug was added to the non-dosing compartment. The study was done in triplicates and repeated once. During the studies, cells were incubated in a shaking incubator at 37^{o}C. At specified time points, 200 µL aliquots were taken from the non-dosing compartment and replaced with fresh medium. Samples were stored at -20^{o}C until analysis by HPLC method.

Preliminary Pharmacokinetics of AG10. Pharmacokinetics of **AG10** in mice were determined by Medicilon. Two sets of 24 ICR mice (19.9 to 28.2 g) were treated with an i.v. bolus injection of **AG10** (in 5% DMSO/20% PEG400/75% saline) at 3 mg/kg or **AG10** orally at 30 mg/kg. Blood samples (approximately 500 µL) were collected via cardiac puncture after euthanasia by carbon dioxide inhalation at 5 min, 15 min, 30 min, 1, 2, 4, 8, and 24 hours post-dose. Plasma samples were the analyzed by HPLC-MS/MS. Chromatography was Zorbax SB-Phenyl column (3.5µm, 2.1*100 mm) eluting at 300 µL/min with 0.1% formic acid in 95% methanol/H_2O. Mass analysis was performed in the positive ion mode on Agilent 6410B. Tolbutamide was used as an internal standard.

Cytotoxicity Assay. $5x10^3$ cells were seeded on 80 μL growth media (except 2.5 x 10^4 Jurkat cells) in each well in 96-well plates and incubate O/N at 37 °C. 20 μL of fresh growth media containing each compound were added into each well to make the final concentration ranging from 1-100 μM. DMSO was used for normalization. Cell titer was tested every 24 h using CellTiter 96 non-radioactive cell proliferation assay kit (Promega, Madison, WI) at 560nm absorbance.

Preliminary evaluation of AG10 toxicity in rats. The *in vivo* toxicity of **AG10** was evaluated in rats. Adult male Wistar rats (Simonsen Laboratories, Gilroy, CA), body weight ranging 160-200 g, were used for the study. In a 28-day toxicity study, five treated and five control rats received a daily dose of **AG10** (50 mg/kg/day of the **AG10** sodium salt solution in water) or placebo dosing (water) by oral gavage, without overnight fasting. The plasma C_{max} of **AG10** after oral dosing with 50mg/kg was ~40 μM. Animals were observed daily and their body weight was measured weekly and used for calculation of the amount of **AG10** to be administered. After 28 days of dosing, the animals were euthanized using a carbon dioxide gas chamber according to the recommendations from the 2007 AVMA Guidelines on Euthanasia and the NIH Guidelines for the Care and Use of Laboratory Animals. Blood samples and other organs (liver, kidney, heart, spleen, thymus, and lungs) were collected during autopsy for further evaluation. All animal protocols were approved by the Animal Care Committee of the University of the Pacific and complied with the Guide for the Care and Use of Laboratory Animals (Eighth Edition, 2011). Comprehensive evaluations of the health status of **AG10** treated and untreated control animals were performed. This evaluation included a clinical chemistry panel of 23 variables (Albumin, Alk. Phosphatase , ALT (SGPT), amylase, AST (SGOT), bicarbonate, total bilirubin, indirect bilirubin, direct bilirubin, BUN, calcium, chloride, cholesterol, CK, creatinine, GGT, LDH, lipase, phosphorus, potassium, total protein, sodium, uric acid) and a complete blood count (CBC) (WBC, RBC, hemoglobin, hematocrit, erythrocyte indices (MCV, MCH, MCHC), reticulocyte count, platelet count, WBC differential, smear evaluation).

Crystallization and Structure Determination of the TTR/Ligand Complexes. WT- and V22I-recombinant mutant TTR proteins were concentrated to 6 mg/mL in 10 mM sodium phosphate buffer and 100 mM KCl (pH 7.6) and co-crystallized at room temperature with a 5 molar excess of tafamidis or **AG10** using the vapor-diffusion sitting drop method. All crystals were grown from 1.395 M sodium citrate, 3.5% v/v glycerol at pH 5.5. The crystals were cryo-protected with 10% v/v glycerol. Data were collected at beam-lines 11-1 or 12-2 at the Stanford Synchrotron Radiation Lightsource (SSRL) at a wavelength of 0.9795 Å. All diffraction data were indexed, integrated, and scaled using XDS in space group $P2_12_12$ with two subunits observed per asymmetric unit. Ligand coordinates and restraints files were generated using the PRODRG server (http://davapc1.bioch.dundee.ac.uk/prodrg/). Ligands were assigned an occupancy of 0.5 to account for their position on the incident 2-fold symmetry axis (z- or C2). Further model building and refinement was completed using Coot and Refmac5. Hydrogens were added during refinement, and anisotropic B-values calculated. Final models were validated using the JCSG quality control server v2.8 (http://smb.slac.stanford.edu/jcsg/QC/) incorporating Molprobity, ADIT (http://rcsb-deposit.rutgers.edu/validate) WHATIF and Resolve. Data collection and refinement statistics are displayed in Table S3. Figure generated using the MOE, Chemical Computing Group, Montreal, Canada.

Portions of this research were carried out at the Stanford Synchrotron Radiation Lightsource, a Directorate of SLAC National Accelerator Laboratory and an Office of Science User Facility operated for the U.S. Department of Energy Office of Science by Stanford University. The SSRL Structural Molecular Biology Program is supported by the DOE Office of Biological and Environmental Research, and by the National Institutes of Health, National Institute of General Medical Sciences (including P41GM103393) and the National Center for Research Resources (P41RR001209).

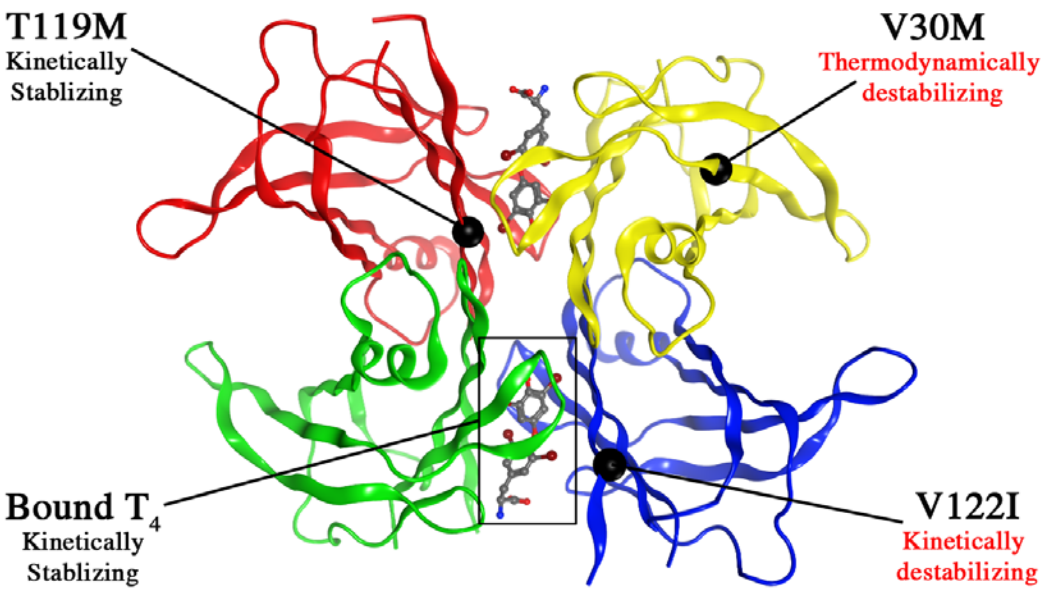

Figure S1. Structure of TTR shown as backbone ribbon representation with each of the monomers individually colored (2ROX)(7). Thyroxine (T_4) shown as ball and stick bound to the two T_4-binding sites kinetically stabilizing the weaker dimer-dimer interface. Black spheres represent the Cα positions of amino-acid mutations that alter the TTR tetramer stability either kinetically or thermodynamically.

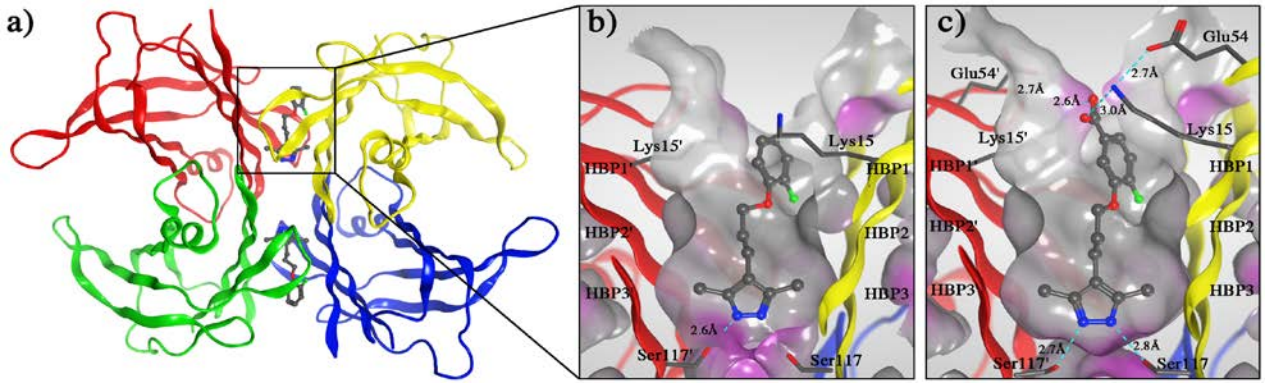

Figure S2. Crystal structures of TTR ligand complexes. (*A*) Quaternary structure of **1** bound to WT-TTR shown as a ribbon representation with monomers colored individually. (*B*) **1** in complex with WT-TTR (3P3T) (6). (*C*) **AG10** in complex with V122I-TTR showing the introduced carboxylate making electrostatic salt bridge interactions with Lys15 and Lys15'. Close-up views of one of the two identical T_4-binding sites in a ribbon depicted tetramer colored by chain. A "Connolly" molecular surface (8) was applied to residues within 10 Å of ligand in the T_4-binding pocket hydrophobic (grey), polar (purple). The innermost halogen binding pockets (HBPs) 3 and 3′ are composed of the methyl and methylene groups of S117/117′, T119/119′, and L110/110′. HBPs 2 and 2′ are made up by the side chains of L110/110′, A109/109′, K15/15′, and L17/17′. The outermost HBPs 1 and 1′ are lined by the methyl and methylene groups of K15/15′, A108/108′, and T106/106′. Hydrogen bonds shown in light blue dashed lines, with the atomic distances labeled in Å. This figure was generated using the program MOE (2011.10), Chemical Computing Group, Montreal, Canada.

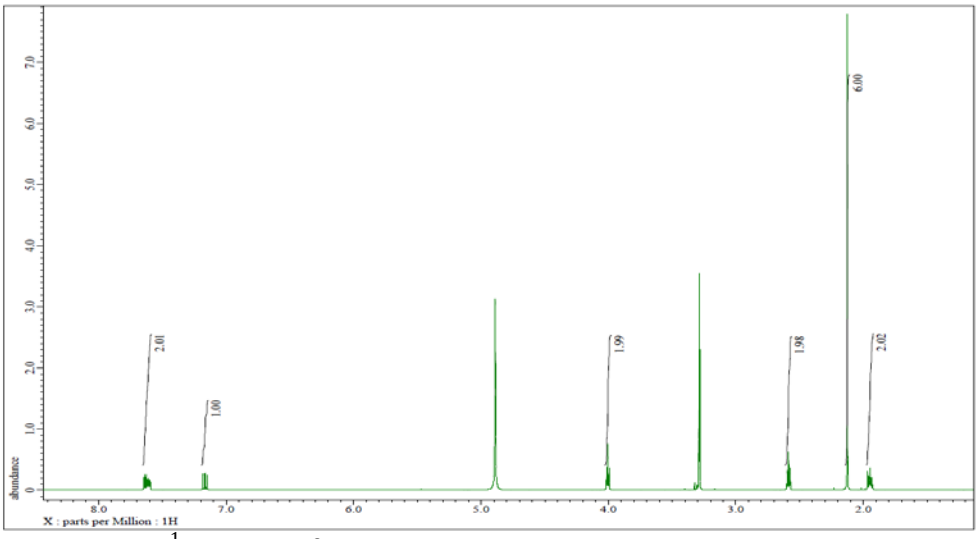

Figure S3A. ^{1}H NMR of **AG10**.

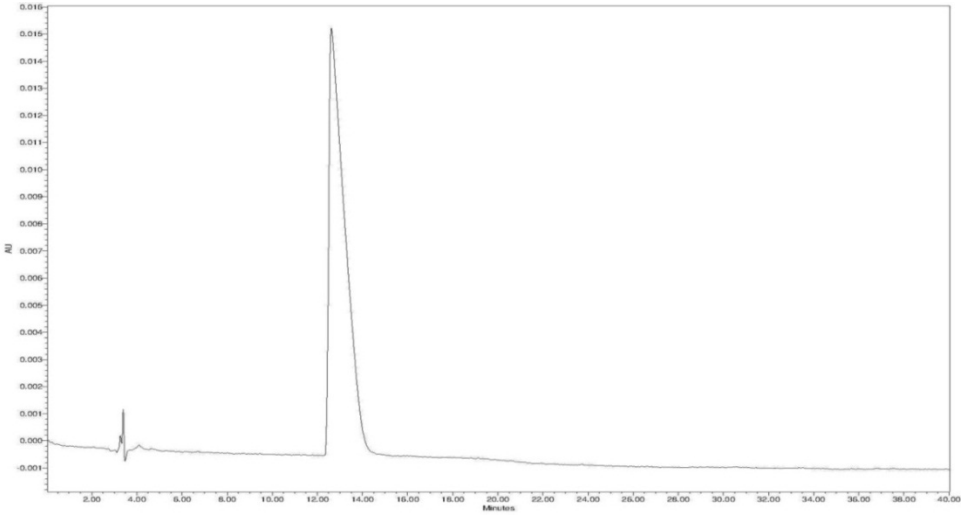

Figure S3B. HPLC trace of **AG10** (>98% purity).

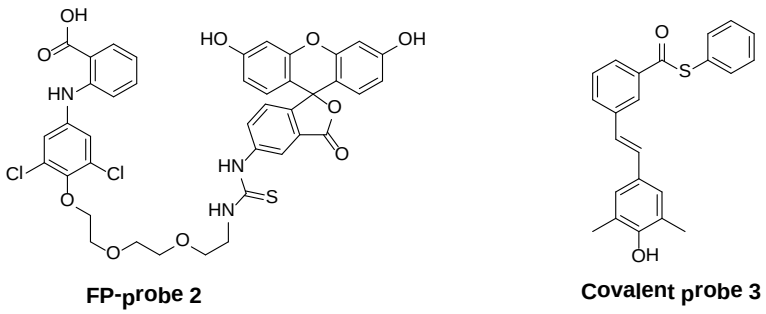

Figure S4. Chemical structures of Fluorescence Polarization (FP)-probe **2** and covalent fluorescence probe **3**.

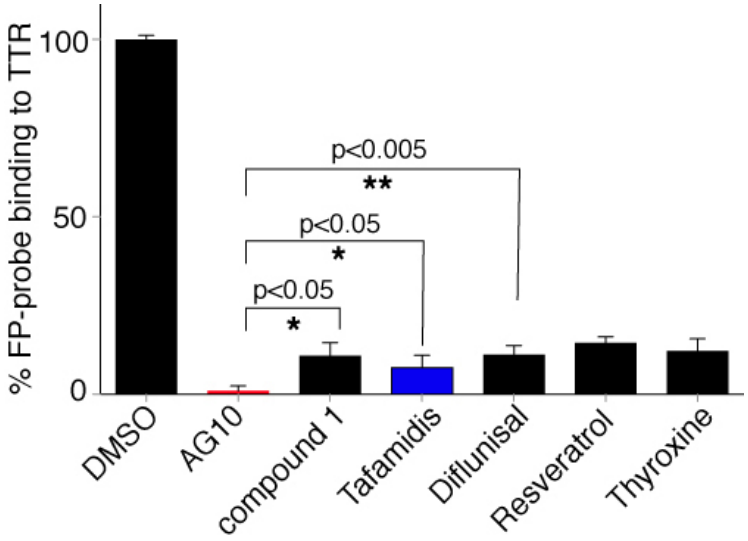

Figure S5. Evaluation of ligand binding to TTR in buffer by fluorescence polarization. TTR ligands (10 μM) competitively displace the FP-probe **2** (0.2 μM) from TTR (0.4 μM) through binding to the T_4-binding sites (the lower the probe binding, the higher the binding affinity of TTR ligand). ** $p<0.005$, * $p<0.03$.

2-(3,5-dichlorophenyl)benzo[d]oxazole-6-carboxylic acid (Tafamidis); synthesized as reported earlier (3). ^{1}H NMR (DMSO-d_6, 600 MHz) δ 8.24 (s, 1H), 8.11 (d, 2H, J = 1.8 Hz), 8.00 (dd, 1H, J_1 = 1.4 Hz, J_2 = 8.3Hz), 7.93-7.86 (m, 2H); HRMS (DART) m/z calcd for $C_{14}H_7Cl_2NO_3$ + H^+ 307.9881; found 307.9891 (M + H^+).

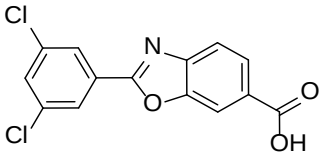

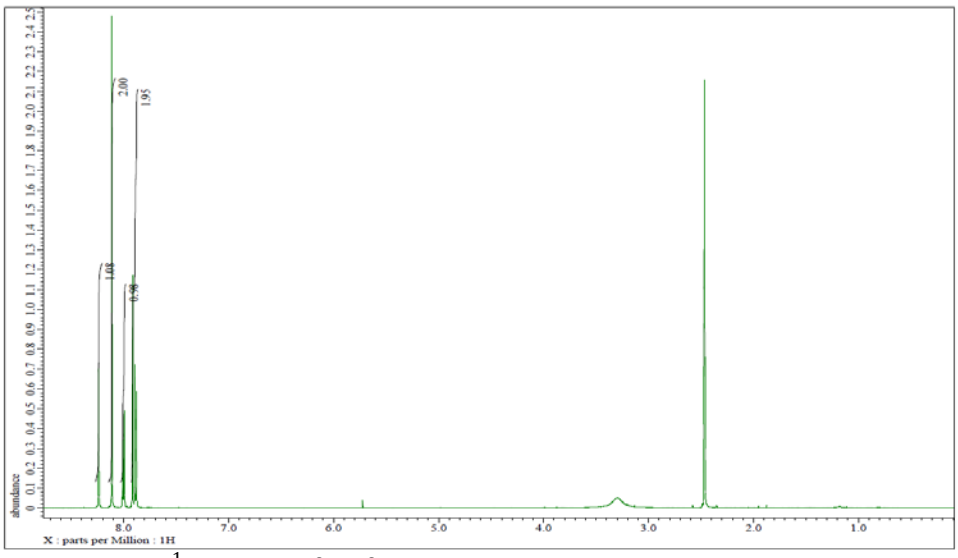

Figure S6A. ^{1}H NMR of Tafamidis.

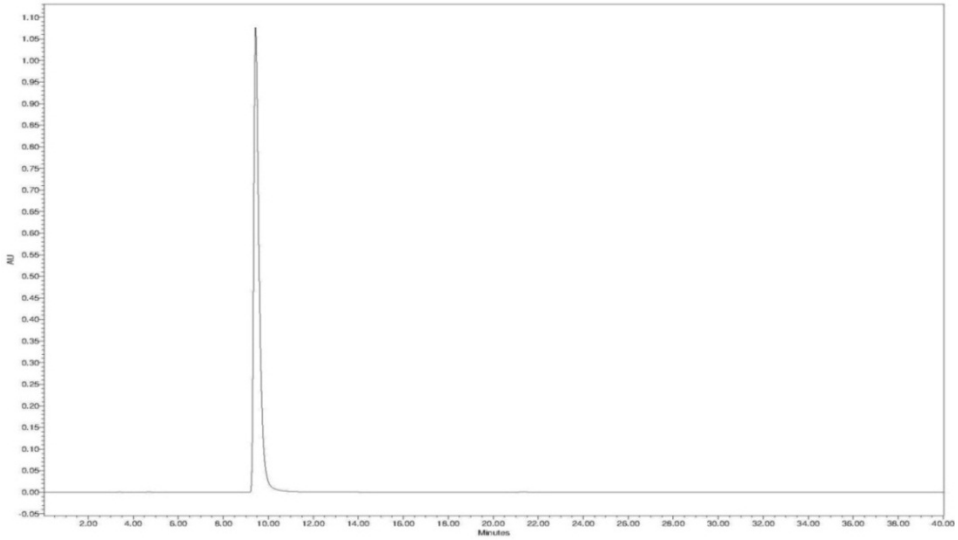

Figure S6B. HPLC trace of tafamidis (>98% purity).

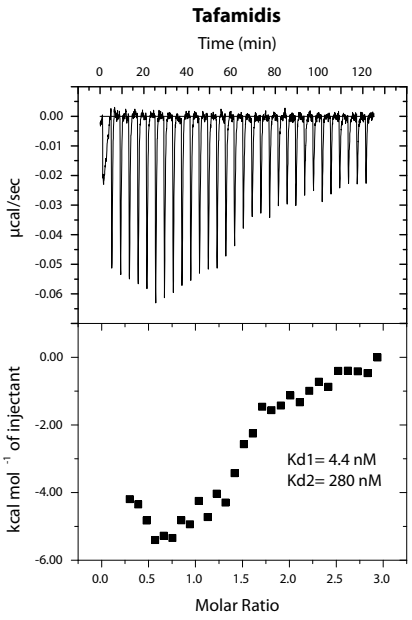

Figure S7. Assessment of the binding affinity of tafamidis to TTR by isothermal titration calorimetry. Calorimetric titration of tafamidis against TTR (K_{d1} = 4.4 nM and K_{d2} = 280 nM). Raw data (top) and integrated heats (bottom) from the titration of TTR (2 µM) with tafamidis (25 µM).

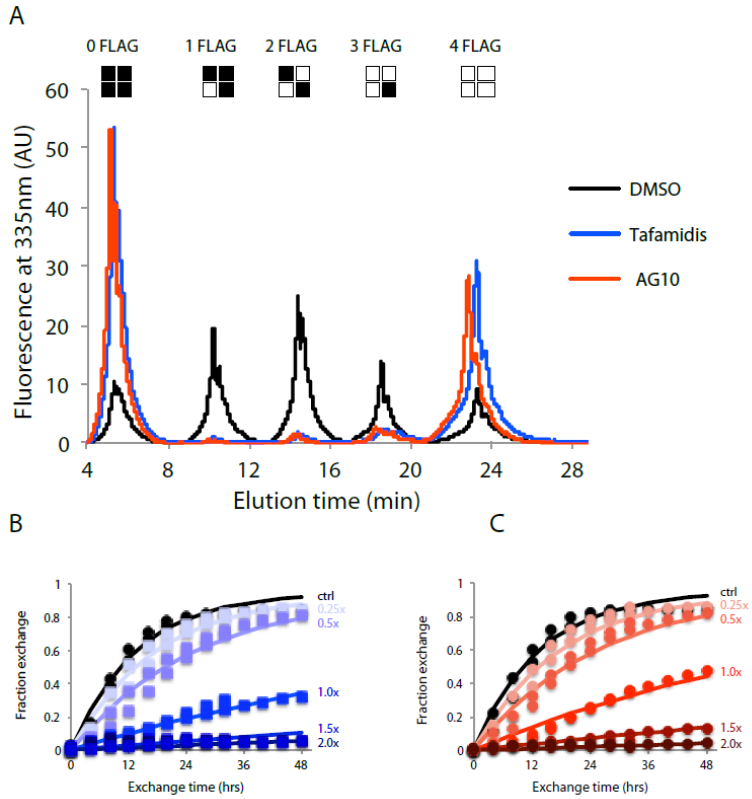

Figure S8. V122I-TTR tetramer stabilization by **AG10** or tafamidis under physiologic conditions, monitored by subunit exchange. (*A*) UPLC traces after 32 h exchange in the presence of 0.9 µM compound (molar ratio of 2:1 compound : tetramers) or vehicle. (*B*, *C*) Dose-dependent stabilization of V122I by tafamidis (*B*) or **AG10** (*C*). At each time point, extent of exchange was calculated by dividing the area of the 2 FLAG peak by the total area under all 5 peaks. The fraction exchange was calculated as (extent of exchange) / 0.375 (see SI Methods). Symbols represent individual data points; curves represent the best fit model to the data.

(E)-S-phenyl 3-(4-hydroxy-3,5-dimethylstyryl)benzothioate (Covalent probe 3); synthesized as reported earlier (4). ^{1}H NMR (DMSO-d_6, 600 MHz) δ 8.44 (s, 1H), 8.03 (m, 1H), 7.90 (d, 1H, J = 7.7 Hz), 7.78 (d, 1H, J = 7.7 Hz), 7.55-7.48 (m, 6H), 7.22-7.10 (m, 4H), 2.16 (s, 6H); HRMS (DART) m/z calcd for $C_{14}H_7Cl_2NO_3$ + H^+ 361.1257; found 361.1260 (M + H^+).

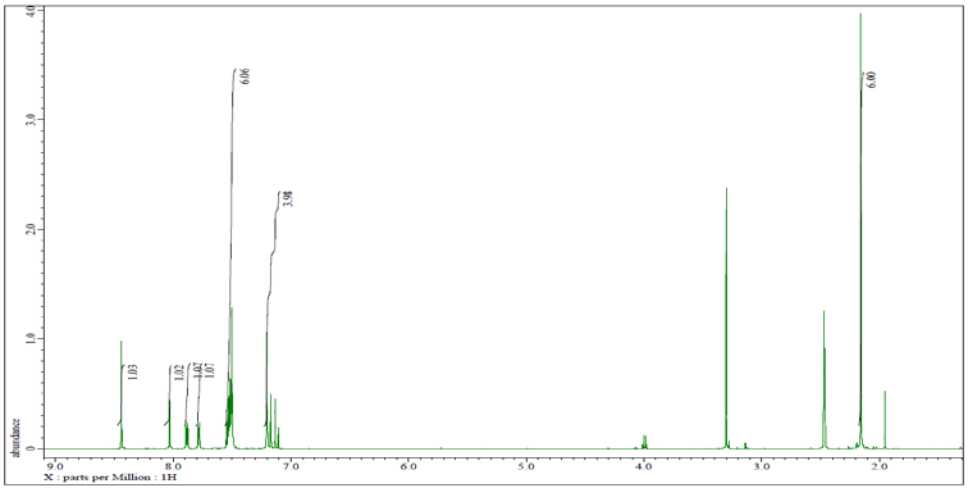

Figure S9. ^{1}H NMR of probe **3**.

A

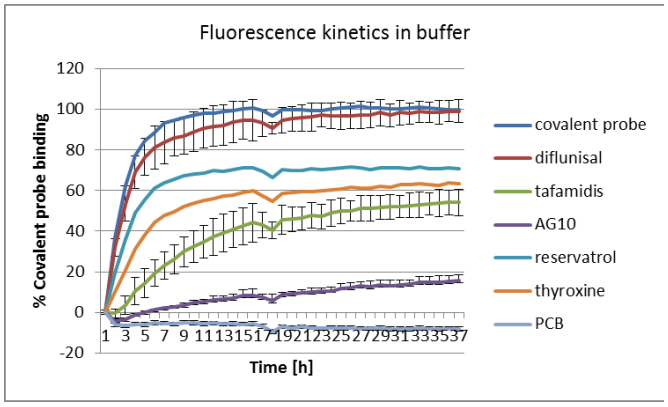

B

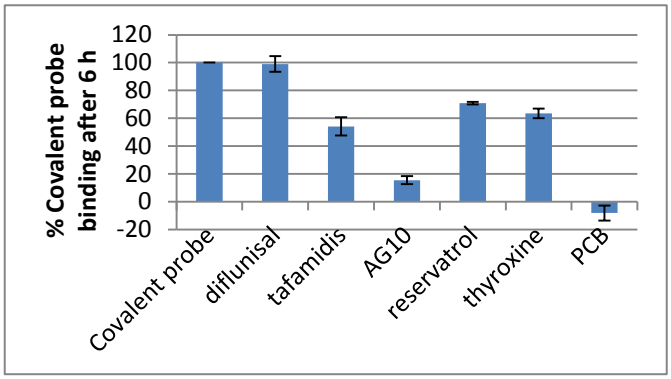

Figure S10. Probe **3** competition assay in with recombinant TTR in buffer **(A)** Fluorescence change due to modification of recombinant TTR (3.6 μM) in buffer by covalent probe **3** monitored for 6 h in the presence of probe alone (3.6 μM) or probe and TTR ligands (10 μM). **(B)** Percentage of covalent probe binding to TTR in the presence of ligands measured after 6 hours of incubation, relative to probe alone. Each bar shows the mean (SD) of three replicates.

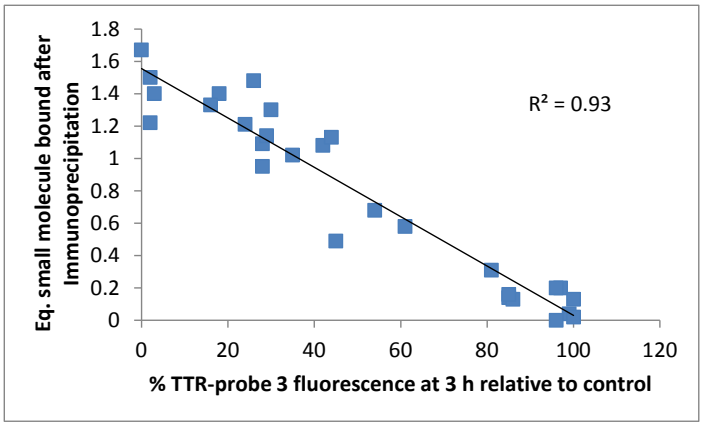

Figure S11. Linear correlation between the extent of TTR–probe **3** conjugate fluorescence after a 3 h competition with latent fluorogenic probe **3** and the previously reported plasma TTR binding stoichiometry data(data are re-plotted from (4))

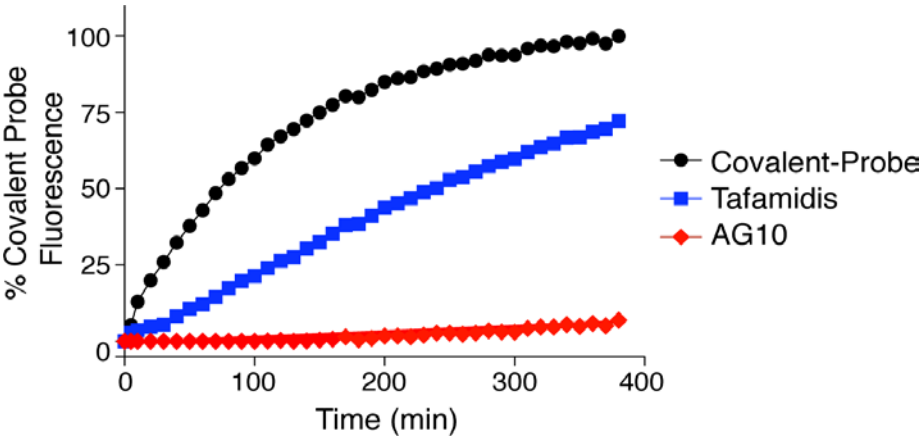

Figure S12. AG10 is selective to V122I-TTR in FAC patient's serum. Fluorescence change due to modification of V122I-TTR in patient's serum by covalent probe **3** monitored for 6 h in the presence of probe alone (black circles) or probe and TTR ligands (colors). Each bar shows the mean (SD) of three replicates.

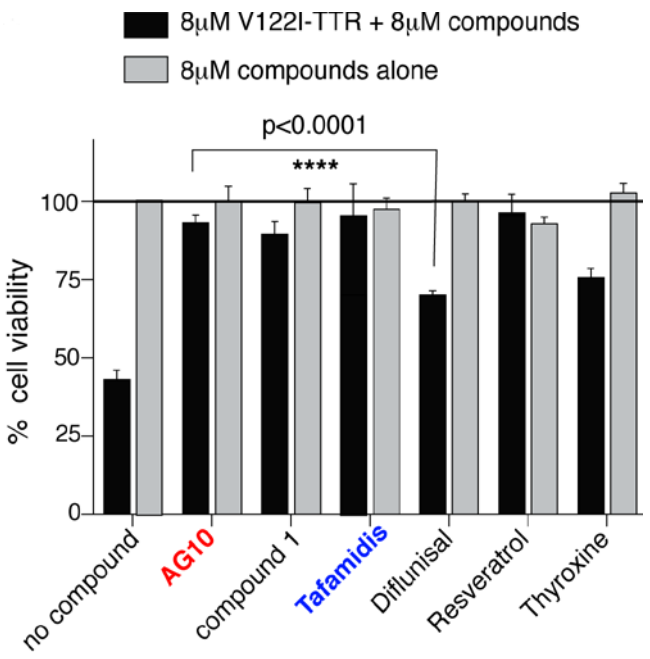

Figure S13. AG10 protects cardiomyocytes from V122I-TTR induced proteotoxicity. Inhibition of V122I-TTR (8 μM) cytotoxicity toward human cardiac AC16 cells by test compounds (8 μM). Cell viability is shown relative to cells treated with vehicle only (100% cell viability). None of the compounds was cytotoxic to the cells at the concentration tested (8 μM). Columns represent the mean of two independently performed experiments (n=8). Error bars, SEM.

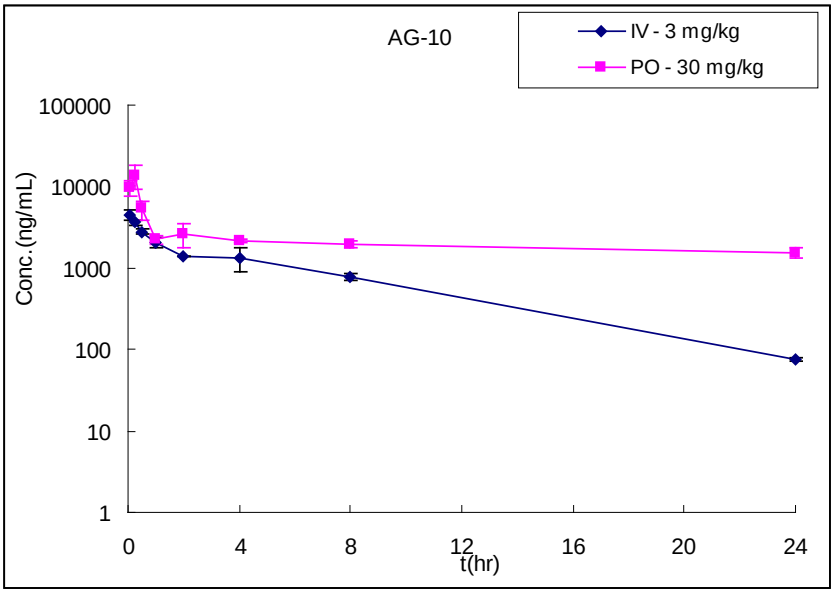

Figure S14. Comparisons of mean concentration-time curve of **AG10** in ICR mice following intravenous injection at 3 mg/kg and oral administration at 30 mg/kg (mean ± SD).

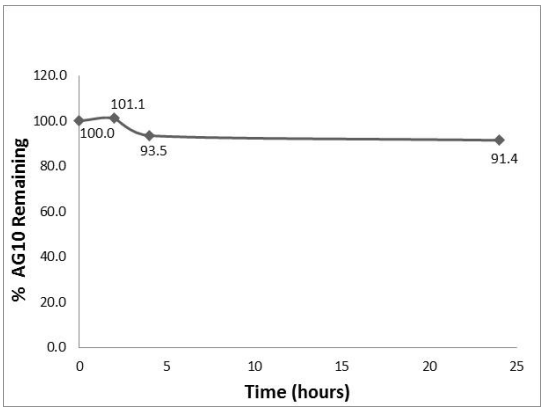

Figure S15. Stability of **AG10** in simulated gastric fluid. **AG10** (20 μM) was added to USP simulated gastric fluid (SGF) and incubated at 37°C in a shaking water bath. Gastric stability study samples (50 μL) were assayed at 0, 2, 4 and 24 hour time intervals. Samples were processed by adding 200 μL methanol followed by centrifuging at 16000 x *g* for 5 min and analyzing the supernatant using the previously described HPLC method.

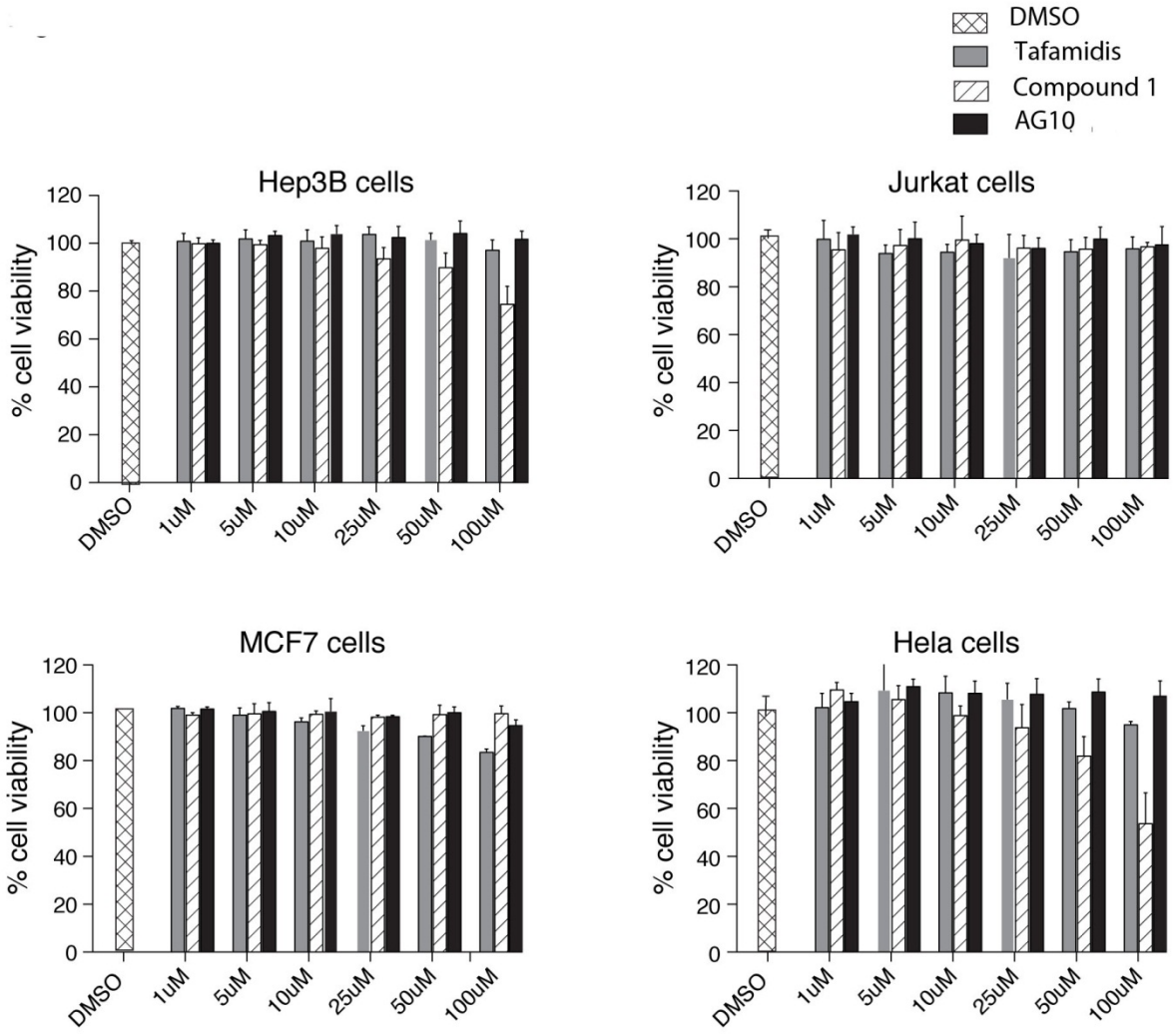

Figure S16. Assessment of the cytotoxicity of tafamidis, compound **1**, and **AG10**, at concentrations from 1 to 100 μM, on a number of cell lines. Hep3B; human hepatoma cell line. Jurkat; T lymphocyte cell line. MCF7; breast cancer cell line. HeLa; cervical cancer cell line Cell viability was assessed using the MTT assay after 24 h. Cell viability results are reported relative to cells treated with vehicle only (100% cell viability). Each bar shows the mean (SD) of three replicates.

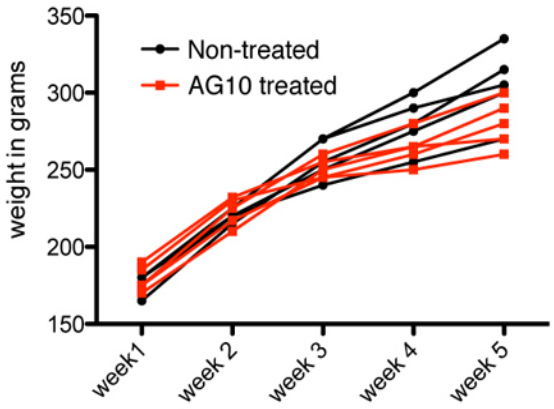

Figure S17. Effect of 28 day AG10 administration on body weight of rats: Individual body weights were recorded before the first administration of AG10 and thereafter weekly. Rats received either **AG10** (50 mg/kg) or water by oral gavage once daily.

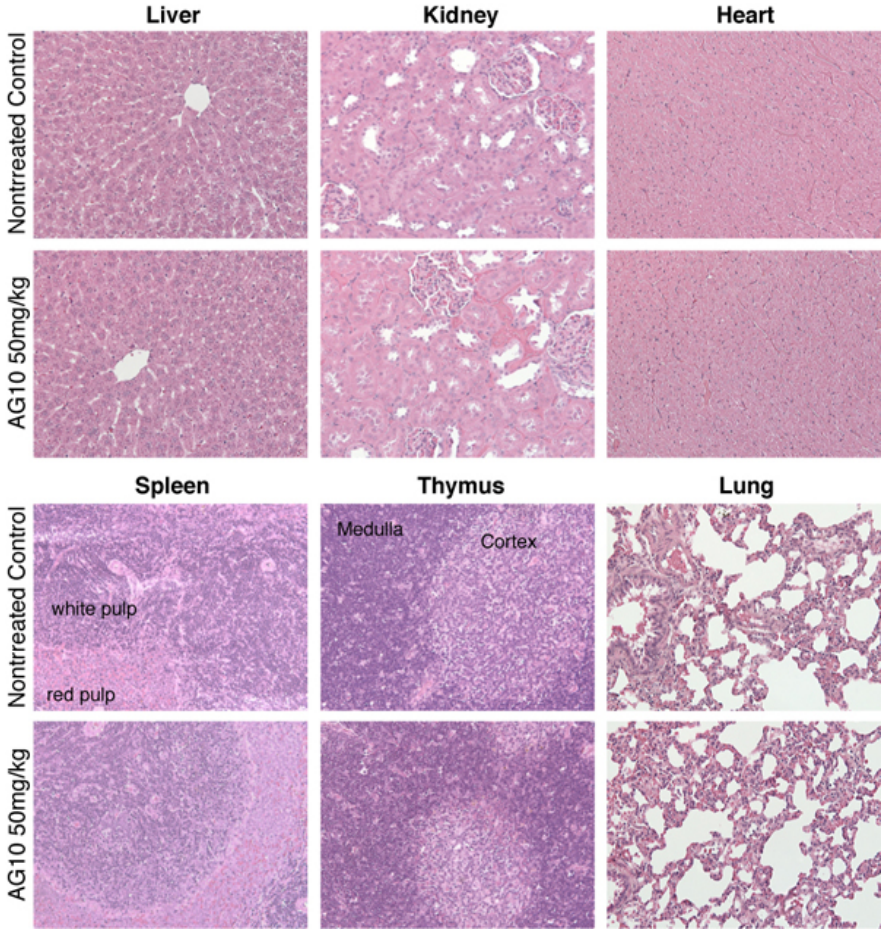

Figure S18. Histopathological examination following a subacute (28 day) toxicity study: Rats received either **AG10** (50 mg/kg) or water by oral gavage once daily. Organs were obtained for histological evaluation by hematoxylin and eosin (H&E) staining.

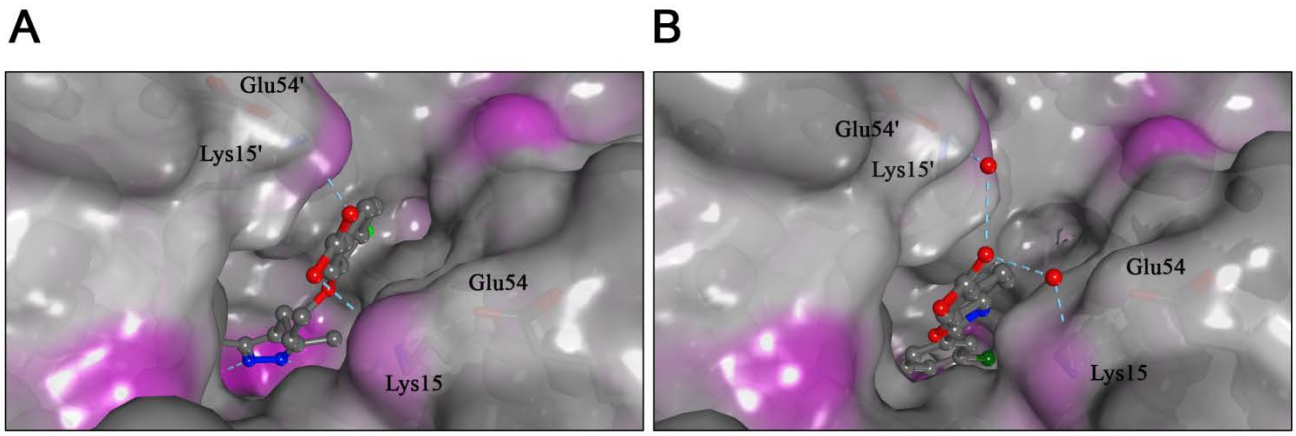

Figure S19. Crystal structures of V122I-TTR ligand complexes. Top view of the T_4 binding pocket with **AG10** (*A*) and tafamidis (*B*) bound respectively, highlighting the change in pocket conformation upon ligand binding. The innermost halogen binding pockets (HBPs) 3 and 3′ are composed of the methyl and methylene groups of S117/117′, T119/119′, and L110/110′. HBPs 2 and 2′ are made up by the side chains of L110/110′, A109/109′, K15/15′, and L17/17′. The outermost HBPs 1 and 1′ are lined by the methyl and methylene groups of K15/15′, A108/108′, and T106/106′. Hydrogen bonds shown in light blue dashed lines, with the atomic distances labeled in Å.

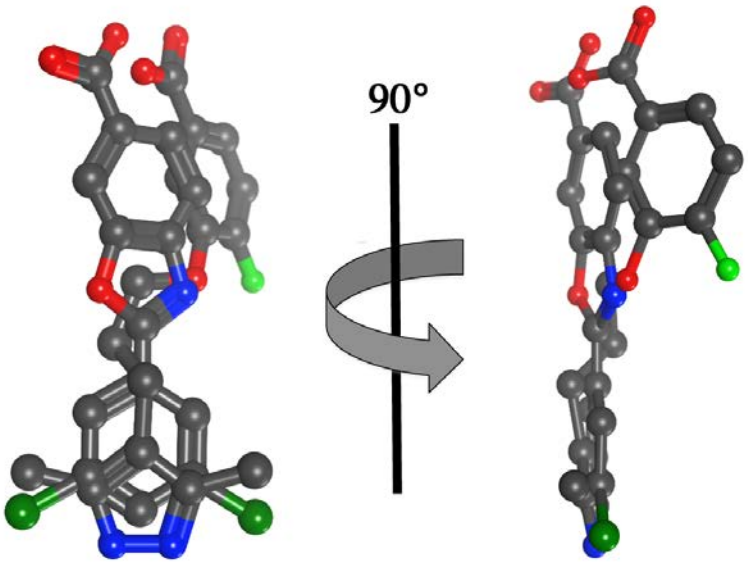

Figure S20. Superposed conformations of **AG10** and tafamidis as bound to V122I-TTR and rotated through 90°.

Table S1. Effect of **AG10** on COX-1, COX-2, THR, hERG, and CYP enzymes.

Target	AG10	Control
COX-1	IC_{50} > 10 μM	Diclofenac (IC_{50} = 0.015 μM)
COX-2	IC_{50} > 10 μM	Diclofenac (IC_{50} = 0.022 μM)
THR	IC_{50} > 10 μM	T3 (IC_{50} = 0.0009 μM)
hERG	IC_{50} > 100 μM	E-4031 (IC_{50} = 0.012 μM)
CYP1A2	IC_{50} > 50 μM	Furafylline (IC_{50} = 6.277 μM)
CYP2C8	IC_{50} > 50 μM	Quercetin (IC_{50} = 0.767 μM)
CYP2C9	IC_{50} > 50 μM	Sulfaphenazole (IC_{50} = 0.235 μM)
CYP2C19	IC_{50} > 50 μM	Tranylcrypromine (IC_{50} = 4.32 μM)
CYP2D6	IC_{50} > 50 μM	Quinidine (IC_{50} = 0.05 μM)
CYP3A4	IC_{50} > 50 μM	Ketoconazole (IC_{50} = 0.016 μM)

Table S2. Selected pharmacokinetics parameters of **AG10** in ICR mice following intravenous injection at 3 mg/kg and oral administration at 30 mg/kg (performed by Medicilon Inc., an FDA approved CRO that is specialized in preclinical evaluation).

Dosage	$t_{1/2}$	T_{max}	C_{max}	$AUC_{(0-t)}$	$AUC_{(0-\infty)}$	Vz	CL	$MRT_{(0-\infty)}$	F*	F**
	hr	hr	ng/mL	ng/mL*hr	ng/mL*hr	L/kg	L/hr/kg	hr	%	%
IV-3 mg/kg	4.79	0.083	4485.37	18571.98	19085.85	1.09	0.16	6.01	-	-
PO-30 mg/kg	42.29	0.25	13771.86	49854.31	143479.66	-	-	58.86	75.18	26.84

*The bioavailability was calculated as F (%) = ($Dose_{iv}$ × $AUC_{po(0-\infty)}$) / ($Dose_{po}$× $AUC_{iv(0-\infty)}$) × 100%.
**The bioavailability was calculated as F (%) = ($Dose_{iv}$ × $AUC_{po(0-t)}$) / ($Dose_{po}$× $AUC_{iv(0-t)}$) × 100%.

Table S3: Data collection and refinement statistics.

	V122I-TTR/AG10	V122I-TTR/Tafamidis
Data Collection		
Beamline	SSRL 11-1	SSRL 11-1
Wavelength (Å)	0.9797	0.9797
Resolution (Å)	1.18 (1.18-1.25)[a]	1.20 (1.20-1.27)[a]
Space group	$P2_12_12$	$P2_12_12$
a, b, c (Å)	42.73, 84.84, 63.91	42.67, 84.60, 64.32
No. of molecules in the a.u.	2	2
No. of observations	459,319 (48,742)[a]	454,519 (59,987)[a]
No. of unique reflections	75,242 (9,986)[a]	73,110 (10,446)[a]
Completeness (%)	98.6 (91.0)[a]	99.6 (98.4)[a]
R_{sym} (%)[b]	2.2 (33.2)[a]	2.8 (55.1)[a]
R_{pim} (%)[c]	1.0 (16.0)[a]	1.2 (24.8)[a]
R_{meas} (%)[d]	2.4 (37.0)[a]	3.0 (60.6)[a]
Average I/σ	34.5 (4.5)[a]	26.0 (3.1)[a]
Redundancy	6.1 (4.9)[a]	6.2 (5.7)[a]
Refinement statistics		
Resolution (Å)	1.18-63.91	1.20-64.32
No. of reflections (working set)	71,412 (4,317)[a]	69,336 (4,959)[a]
No. of reflections (test set)	3,769 (234)[a]	3,679 (236)[a]
R_{cryst} (%)[e]	16.0 (24.0)[a]	15.3 (23.6)[a]
R_{free} (%)[f]	18.6 (26.0)[a]	17.2 (25.5)[a]
No.TTR/ligand/water atoms		
Average B-values (Å^2)		
TTR	13.9	14.7
Ligand	13.8	15.5
Wilson B-value	12.9	13.8
Ramachandran plot		
Most favored (%)	99.1	99.6
Additionally allowed (%)	0.9	0.4
R.M.S deviations		
Bond lengths (Å)	0.17	0.17
Angles (°,)	1.73	1.75

[a] Numbers in parentheses are for highest resolution set of data.

[b] $R_{sym} = \sum_{hkl} \left| I - \langle I \rangle \right| \sum_{hkl} I$

[c] $R_{meas} = \sum_{hkl} [N/(N-1)]^{1/2} \sum_i \left| Ii(hkl) - I(hkl) \right| / \sum_{hkl} \sum_i Ii(hkl)$

[c] $R_{p.i.m} = \sum_{hkl} [1/(N-1)]^{1/2} \sum_i \left| Ii(hkl) - I(hkl) \right| / \sum_{hkl} \sum_i Ii(hkl)$

[e] $R_{cryst} = \sum_{hkl} \left| F_o - F_c \right| \sum_{hkl} F_o$

[f] R_{free} is the same as R_{cryst} but for 5% of data excluded from the refinement.

References:

1. Purkey HE*, et al.* (2004) Hydroxylated polychlorinated biphenyls selectively bind transthyretin in blood and inhibit amyloidogenesis: rationalizing rodent PCB toxicity. *Chem Biol* 11:1719-1728.
2. Razavi H*, et al.* (2003) Benzoxazoles as transthyretin amyloid fibril inhibitors: synthesis, evaluation, and mechanism of action. *Angew Chem Int Ed Engl* 42:2758-2761.
3. Bulawa CE*, et al.* (2012) Tafamidis, a potent and selective transthyretin kinetic stabilizer that inhibits the amyloid cascade. *Proc Natl Acad Sci U S A* 109:9629-9634.
4. Choi S & Kelly JW (2011) A competition assay to identify amyloidogenesis inhibitors by monitoring the fluorescence emitted by the covalent attachment of a stilbene derivative to transthyretin. *Bioorg Med Chem* 19:1505-1514.
5. Bourgault S*, et al.* (2011) Mechanisms of transthyretin cardiomyocyte toxicity inhibition by resveratrol analogs. *Biochem Biophys Res Commun* 410:707-713.
6. Alhamadsheh MM*, et al.* (2011) Potent kinetic stabilizers that prevent transthyretin-mediated cardiomyocyte proteotoxicity. *Sci Transl Med* 3:97ra81.
7. Wojtczak A, Cody V, Luft JR, & Pangborn W (1996) Structures of human transthyretin complexed with thyroxine at 2.0 A resolution and 3',5'-dinitro-N-acetyl-L-thyronine at 2.2 A resolution. *Acta Crystallogr D Biol Crystallogr* 52:758-765.
8. Connolly ML (1983) Solvent-accessible surfaces of proteins and nucleic acids. *Science* 221:709-713.